Purification and Characterization of BaeI and PksL in Bacillus amyloliquefaciens and Analysis of Protein Activity within the Bacillaene and Difficidin clusters of Bacillus Subtilis

By: Alexis Lewars

Principal Investigator: Dr. Jason Reddick

Contributors: Dr. Jason Reddick, Robert Tikkanen, Dr. Brittany Kiel, Victoria Meadows, and Don Mora

Abstract

In these experiments, the genes PksL and BaeI were purified and cloned into vectors such as Top10 and BL21 star. SDS-Page and Gel electrophoresis were used to confirm the transformation of these genes. The sequence of BaeI was confirmed through Sanger sequencing. A reaction of PksL with CoA and Sfp was run to determine the successful addition of the phosphopantetheine arm to the acyl carrier protein. Bacillaene and Difficidin were assigned homologs by structural and genetic analysis using protein sequencing provided by NCBI. The sequences of such amino acids were analyzed for distinct characteristics. Future experiments within the Reddick laboratory will involve reactions with BaeI and PksL to determine double bond placement within Difficidin polyketide synthesis.

Introduction

Bacillus Amyloliquefaciens are a species of gram-positive bacterium that are located within the rhizosphere of soil. Bacillus Amyloliquefaciens are responsible for allowing plants to survive in a variety of climates by suppressing bacteria and fungi for the plant. This can allow the plant to thrive despite possible threats in the surrounding environment. [1]

Within Bacillus Amyloliquefaciens, many genes can be studied including BaeI and PksL. BaeI and PksL are both genes involved in polyketide synthesis. Polyketide synthesis is the

process by which a group of enzymes may form a polyketide through various reactions. These reactions include dehydration reactions, cyclization reactions, and the removal of CO_2. [2]

While many polyketide synthesis pathways can occur, the particular pathway observed through PksL and BaeI is the process in which a double bond is formed in the structure of Difficidin. This double bond is known as a beta-branch within polyketide synthesis. It is unknown how the two isomers of the Difficidin enzyme are created. This is shown in figure 1. Within these experiments, the proteins were purified to run the reactions to determine how each gene contributes to the creation of bonds. Figure 2 shows the reaction ran so far to determine the effect of PksL on the Acyl Carrier Protein. The reaction in figure 2 is still in the process of being analyzed.

Double Bond Formation in Difficidin Polyketide Synthesis

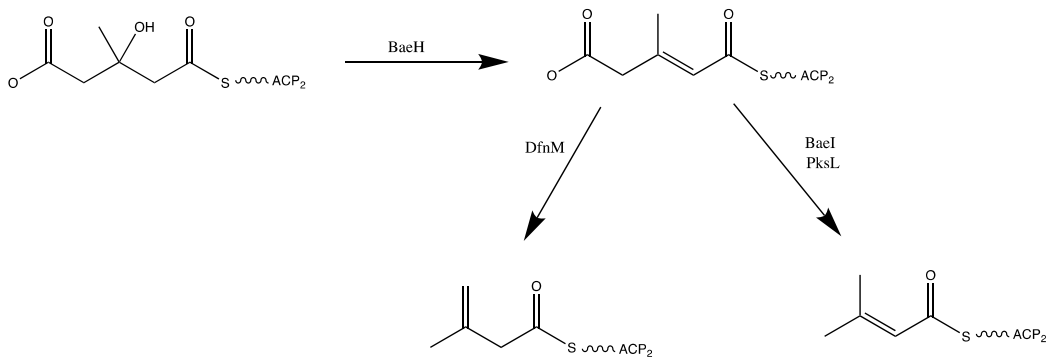

Figure 1: Polyketide Synthesis Pathway for Difficidin involving PksL and BaeI

Reaction of Acyl Carrier Protein and CoA

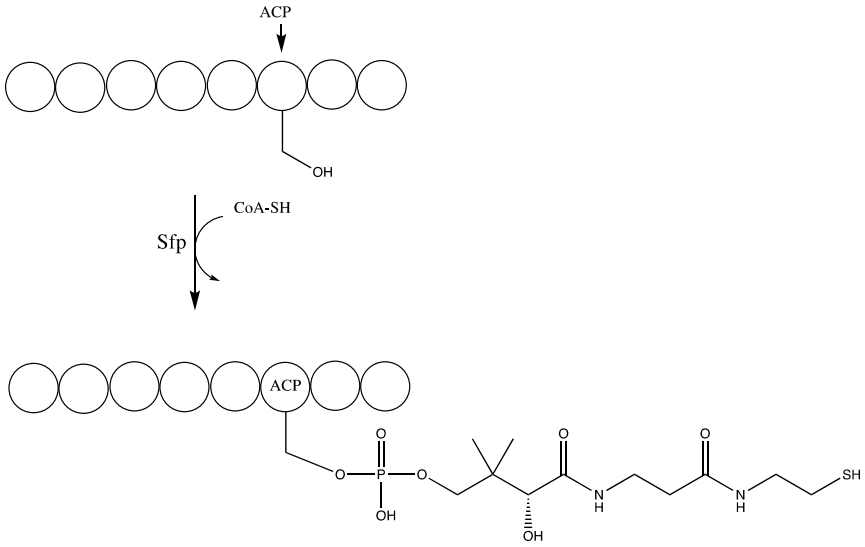

Figure 2: Reaction of Acyl Carrier protein reacting with CoA and Sfp.

The beta-branch formation may be divided into the Difficidin and Bacillaene types such that their sequences may be analyzed. This allows the assignment of homologs of each distinct type of polyketide. This, in theory, would give insight into why these two distinct types of bonds are formed and what is essential within the amino acid to create such bonds.

Experimental

BaeI

Primer Design of BaeI

BaeI primers were designed following the DNA sequence of BaeI on subtilist genolist. The forward primer was designed to hold a sequence of 5'-CAC CAT GCC GAA CGC CGC AGT TG-3' with a TM temperature of 65.6 ℃. The reverse primer was designed to hold a sequence of 5'-TTA TAC TCC GTA CAT CGT CGT GAT TCG TTT TTT CAC-3'with a TM temperature of 60.9℃. TM temperature was determined through the use of the TM calculator by New England Biolabs.

PCR and Genomic DNA Purification for BaeI

Colonies of DNA from Bacillus Amyloliquefaciens from ATCC culture collection 39374 were inoculated and grown to create a small culture. Kanamycin was added to the mixture and the culture was shaken overnight at 37℃. The sample was purified through the use of the Wizard Genomic DNA Purification kit with the steps for gram-positive bacteria. Upstream primer, downstream primer, ddH2O, master mix, and Genomic DNA was added to run PCR on the purified genomic DNA. The temperatures used were as follows: denaturation at 98℃, annealing at 60℃, and Extend and Final Extension at 72℃. An Agarose gel was created with TAE Buffer, Agarose, and Ethidium Bromide. (10 mg/ml). Gel electrophoresis was run at 110 mV with Gel Loading Dye Purple used and a 0.1-10 kb DNA Ladder. Purified Genomic DNA was compared against Genomic DNA purified by a Graduate student, Robert Tikkanen within the lab.

Transformation of BaeI into Top10 Vector

Genomic DNA from PCR, salt solution, H2O, and Topo vector were mixed and incubated for five minutes. This mixture was added to the Top 10 chemically competent E Coli and mixed. The mixture was incubated for 5-30 minutes and heat-shocked at 42℃ for 30 seconds. The mixture was placed on ice and SOC medium at room temperature was added. The mixture was shaken at 200 rpm and 37℃ for an hour. This was spread on plates with 100-200 uL of the mixture and incubated overnight at 37℃. Small cultures were created using Kanamycin, LB broth, and a sample of several of the colonies that grew. Qiapen miniprep plasmid isolation kit was used and Gel Electrophoresis was performed using an Agarose gel created with TAE Buffer, Agarose, and Ethidium Bromide. (10 mg/ml). This was compared against a 2-log DNA ladder. After analyzing the colonies there was a positive transformation.

Sequencing of BaeI

Another sample of the colony that held a positive transformation was grown with a small culture and was purified with the Qiapen miniprep plasmid isolation kit. Then the sample was prepared for Sanger Sequencing by dehydrating the sample with a speed vacuum and adding water to make it a proper concentration.

Transformation of BaeI into BL21 Star Vector

The purified sample of the protein in the Top 10 vector was added to BL21 Star cells. The mixture was stirred and incubated on ice for 30 minutes. The cells were heat-shocked at 42℃ for 30 seconds and placed on ice for 2 minutes before SOC medium was added. The tube of cells was shaken at 200 rpm for 1 hour at 37℃. Two LB-Agar plates were used containing Kanamycin and cells from transformation were added. The plates were incubated overnight at 37℃. Small cultures of several colonies were created a starter culture was created with a volume of 5 mL. This starter culture was used with kanamycin to create a larger culture of 1000 mL. When the culture reached an absorbance of 0.5-0.6, the culture was induced with IPTG (.238 g). This process was interrupted due to a timing issue within the semester and a new group of colonies was grown by using a gel stock of the Genomic DNA in the Top10 Vector within the -80℃ freezer. A small and large culture was made, and the large culture was induced with IPTG (.238 g). The culture shook overnight at 37˚C at 210rpm. The large culture was centrifuged the following day at 6,500 rpm using a JA-10 rotor and the supernatant was disregarded.

Column and SDS Page of BaeI

The pellet created due to centrifugation was suspended using 15 mL of 1X Binding Buffer. The cells were then lysed using sonication while the solution was on the ice. Next, the cells were centrifuged at 11,500 rpm with the JA-20 rotor. The resulting supernatant was filtered

using a 0.45 um sterile syringe filter. This solution was added to a nickel column once the column was prepped with 3 column volumes of ddH20, 5 column volumes of 1x charge buffer, and 3 column volumes of 1x binding buffer. Once the binding buffer reached the top of the bed, the filtered supernatant was added. This was washed with 10 column volumes of 1x binding buffer and 6 column volumes of 1x wash buffer. Next, the protein was eluted using 6 volumes of 1x elute buffer.

The eluted protein was collected and tested with Bradford reagent to determine the presence of protein. This is shown by a color change of brown to blue. Dialysis was performed on the fractions that contained protein using Tris and H_2O calibrated to a pH of 8. 10% glycerol stocks of the resulting protein solution were created using an 80% glycerol stock.

PksL

Transformation of PksL into BL21 Star

A PksL stock solution transformed into Top10 cells from the Walsh lab was added to a sample of BL21 Star cells. Next, the mixture was stirred and incubated on ice for 30 minutes. The cells were heat-shocked at 42℃ for 30 seconds and placed on ice for 2 minutes before SOC medium was added. The tube of cells was shaken at 200 rpm for 1 hour at 37℃. Two LB-Agar plates were used containing Kanamycin and cells from transformation were added. The plates were incubated overnight at 37℃. One of the colonies was used to create a starter culture with a volume of 5 mL. A large culture was created with Kanamycin and the small culture and induced with IPTG (.238 g) when the culture reached an absorbance of .5-.6. The mixture was shaken overnight at 15˚C at 210rpm. The large culture was centrifuged at 6,500 rpm using a JA-10 rotor and the supernatant was disregarded.

Column and SDS Page of PksL

The pellet created due to centrifugation was suspended using 15 mL of 1X Binding Buffer. The cells were lysed with sonication while on ice. Next, the cells were centrifuged with a JA-20 rotor at 11500 rpm. The resulting supernatant was filtered using a 0.45 um sterile syringe filter. This solution was added to a nickel column once the column was prepped with 3 column volumes of ddH20, 5 column volumes of 1x charge buffer, and 3 column volumes of 1x binding buffer. Once the binding buffer reached the top of the bed, the filtered supernatant was added. This was then washed with 10 column volumes of 1x binding buffer and 6 column volumes of 1x wash buffer. Next, the protein was eluted using 6 volumes of 1x elute buffer.

The eluted protein was collected and tested with Bradford reagent to determine the presence of protein. This is shown by a color change of brown to blue. Dialysis was performed on the fractions that contained protein using Tris and H20 calibrated to a pH of 8. 10% glycerol stocks of the resulting protein solution using an 80% glycerol stock.

Reaction of PksL with CoA

A small culture of the PksL protein within BL21 Star was created and ran in a reaction with Sfp, CoA, and $MgCl_2$ buffer (12.5 mM). The mixture was quenched the following day with urea and the reaction was run for an hour before CaCl2 and trypsin was added. The mixture was incubated at 37 ˚C and was measured using the Orbitrap.

Discovery of Similar Polyketides

Literature research was conducted to find papers in which compared similar families of polyketides. From these papers, structures were analyzed, and beta-branches were located. Beta-branches were sorted by appearing similar to the Bacillaene type, Difficidin type, or a new branch type completely.

Analysis of Bacillaene and Difficidin Beta-Branch Homologs

Bacillaene and Difficidin Homologs were analyzed using Global alignment and allow ends to slide alignment within Bioedit. Similarities percentages, identity percentages, and alignment scores were recorded on Excel. Through structural analysis and Bioedit data analysis, the sorting of Bacillaene and Difficidin type beta branching groups were established. Groups were each run through analysis using ClustalW to find locations of interest. Distinct areas were investigated future through additional ClustalW alignments.

Results and Discussion

Figure 3 shows the gel electrophoresis of the genomic DNA of BaeI. The BaeI sample is the sample the experimenter purified and the positive control was the Genomic DNA of BaeI that Robert Tikkanen, a graduate of the Reddick lab, purified. While the purification of the experimenter did not show a band in the correct location, the band of Robert Tikkanen's DNA had a band at approximately 750 bp. This supports that this is the gene desired.

Gel Electrophoresis of BaeI Genomic DNA

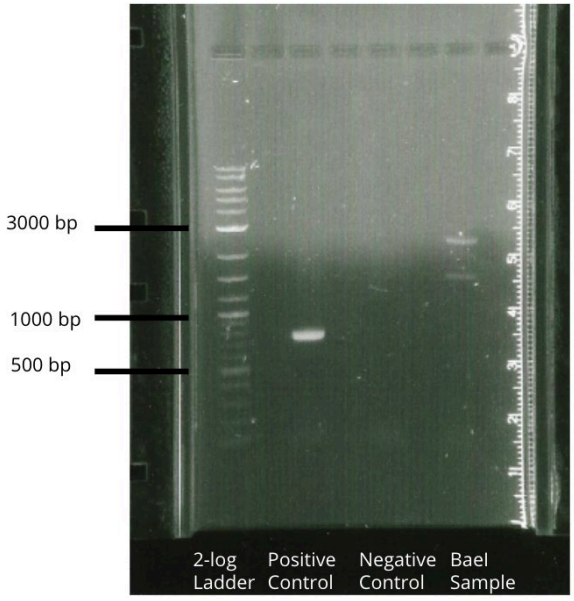

Figure 3: Gel Electrophoresis of BaeI Genomic DNA

Figure 4 shows the experimenter's first attempt at cloning BaeI into the Top10 vector. This is an example of when the ladders did not appear when completing gel electrophoresis. This likely occurred due to a pipetting error and there was another gel electrophoresis ran after this instance.

Gel Electrophoresis of First Attempt Cloning BaeI in Top10 Vector

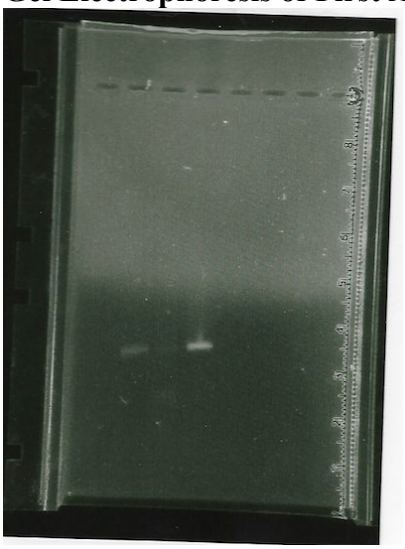

Figure 4: Gel Electrophoresis of unsuccessful Gel Electrophoresis of BaeI Top10 Vector Cloning

Figure 5 shows the Top10 Cloning of BaeI with Genomic DNA isolated from Robert's sample. Lanes 3,5,6 and 7 are 4 colonies that were tested to see if they held BaeI based on the number of base pairs. The positive control was the Genomic DNA Robert isolated. The band in lane 5 was at the same location as the positive control indicating it held the gene. A restreak of this colony was used in BL21 Star cell cloning.

Gel Electrophoresis of BaeI in Top10 Vector

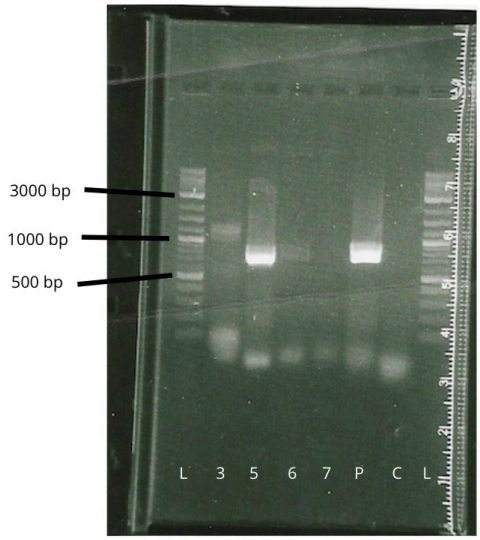

Figure 5: Gel electrophoresis of BaeI cloned into Top10 Vector

Figure 6 shows the SDS-Page of BaeI cloned into BL21 Star vector. The lanes labeled ”S” are those with the cloned DNA. The band appeared between 30,000 and 40,000 daltons which were expected when comparing the number of Daltons in the gene. This allowed for the confirmation of the band is equivalent to the location of BaeI.

SDS-Page of BaeI

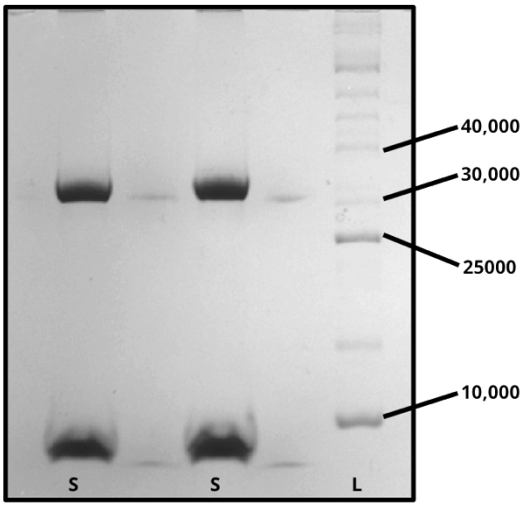

Figure 6: SDS Page of BaeI with 200 kDa Ladder

Figure 7 shows the SDS-Page of PksL. The columns labeled “s” are the samples of PksL cloned into the BL21 Star vector. The molecular weight according to the gel would be between 30,000 and 40,000 Daltons. This was equal to the value expected from Walsh’s lab for the molecular weight of this gene. This confirms PksL was cloned into the PksL vector.

SDS Page of PksL in BL21 Star Vector

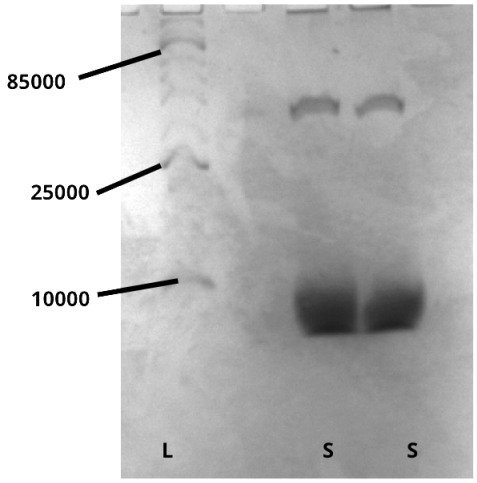

Figure 7: SDS Page of Pksl cloned into the BL21 Star Vector

Figure 8 shows the genes found within Beta-Branching Polyketides found responsible for beta branching within their distinct polyketide. Genes are organized according to if they hold Bacilliaene, Difficidin, or other types of beta branches to then perform further analysis into only Bacillaene and Difficidin types.

Division of Genes responsible for Beta Branching divided into Bacillaene, Difficidin, and Other Types

Bacillaene-Type Beta Branch	Difficidin-Type Beta Branch	Other-Type Beta Branch
BaeI	DfnM	JamJ
MupK	PedI	BryR
OccJ	OnnB	CurF
	DipP	PhmE
	PsyD	PhmI

Figure 8: Bacillaene, Difficidin, and Other Types of Genes responsible for Beta-Branching in Polyketides

Figure 9 shows the genes in which are homologs to Difficidin or Bacillaene. The red box contains the homologs to Difficidin which are Onnamide, Psymberin, Diaphorin, and Pederin. The blue box contains the homologs to Bacillaene which are Oocydin A and Mupirocin. The beta branches of these molecules are marked via ovals on the structure.

Bacillaene and Difficidin Homologs

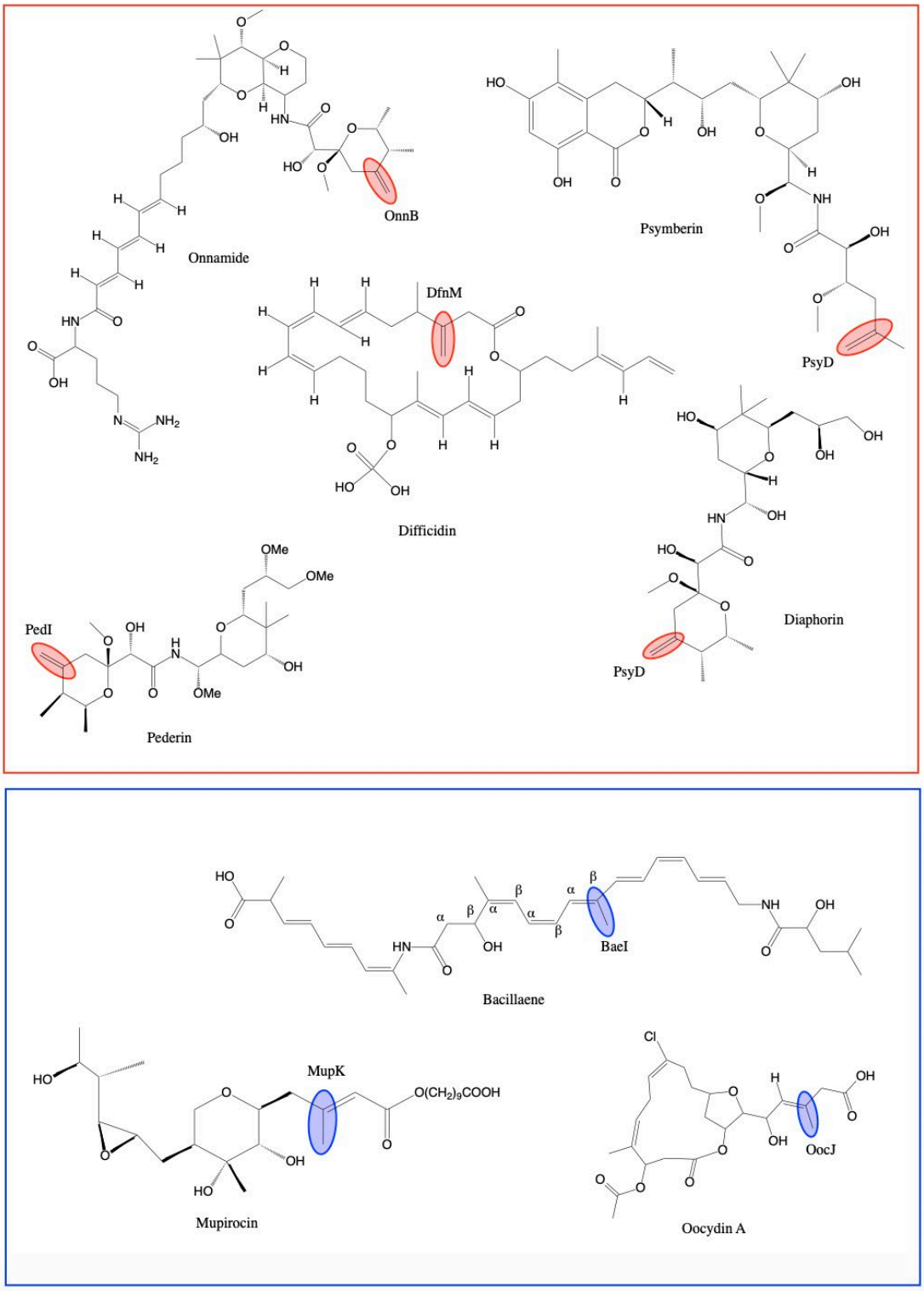

Figure 9: Bacilliene and Difficidin Homologs

Figure 10 shows the Global Alignment of DfnM to all of the genes discovered that were responsible for beta-branch formation. Higher identity, similarity, and alignment scores indicate that the sequences are more similar to one another. Global alignments in conjunction with structural analysis allow for the determination of homolog structures. For DfnM, Onnamide, Psymberin, Diaphorin, and Pederin were determined to be homologs. However, Psymberin despite having a similar beta branch held a very low alignment score symbolizing it was the weakest homolog of the group. Allowing ends to slide alignment was also performed but matched the same pattern for identity, similarity, and alignment scores.

Global Alignment to DfnM

Name	Alignment Score	Identities	Similarities
MupK	657	0.5120968	0.6854839
BryR	-225	0.1505882	0.2941176
BaeI	711	0.562249	0.7148594
PedI	473	0.4189723	0.5849802
PhmE	482	0.4246032	0.6031746
OccJ	471	0.412	0.58
CurF	561	0.4422311	0.6653386
JamJ	565	0.4527559	0.6732283
OnnB	424	0.3636364	0.5731225
DipP	472	0.4047619	0.5992063
PhmI	483	0.416	0.58
PsyD	-34	0.1590909	0.344697

Figure 10: Global Alignment of Beta Branching Genes to the DfnM gene sequence

Figure 11 shows the Global Alignment of BaeI to all of the genes discovered that were responsible for beta-branch formation within different polyketides. Higher identity, similarity, and alignment scores indicate that the sequences are more similar to one another. Global alignments in conjunction with structural analysis allow for the determination of homolog structures. For BaeI, Oocydin A and Mupirocin were determined to be homologs. Allowing ends

to slide alignment was also performed but matched the same pattern for identity, similarity, and alignment scores.

Global Alignment to BaeI

Name	Alignment Score	Identities	Similarities
MupK	730	0.5783133	0.7269076
BryR	-211	0.1738095	0.2833333
DfnM	711	0.562249	0.7148594
PedI	544	0.4347826	0.6166008
PhmE	523	0.4342629	0.6095618
OccJ	530	0.436	0.612
CurF	610	0.46	0.696
JamJ	602	0.476378	0.6850394
OnnB	522	0.4189723	0.6245059
DipP	543	0.4206349	0.6587302
PhmI	583	0.4701195	0.6533865
PsyD	25	0.1811321	0.3584906

Figure 11: Global Alignment of Beta Branching Genes to the BaeI gene sequence

Figure 12 shows the amount of exact, strong, or weak group alignments found through the ClustalW computer software when analyzing the sequence of DfnM and BaeI to the Difficidin Homologs. The sequence of BaeI was more similar in sequence to the DfnM homologs than DfnM itself. However, DfnM held a more similar beta branch in structural analysis. With the exclusion of PsyD, both DfnM and BaeI held a more similar alignment to the DfnM homologs.

DfnM and BaeI Compared to other DfnM Homologs

with and without Exclusion of PsyD

	Exact Alignments	Strong Group Alignments	Weak Group Alignments
w/ PsyD			
Compared to DfnM	6	33	26
Compared to BaeI	10	22	28
w/o PsyD			
Compared to DfnM	71	53	35
Compared to BaeI	75	56	32

Figure 12: DfnM and BaeI Compared to DfnM Homologs within Figure 9

with and without Exclusion of PsyD

Figure 13 shows the exact, strong group, and weak group alignment scores of DfnM and BaeI when compared to the BaeI homologs using the ClustalW computer software. BaeI was closer aligned to the other BaeI homologs than DfnM.

DfnM and BaeI Compared to BaeI Homologs

	Exact Alignments	Strong Group alignments	Weak Group Alignments
BaeI homologs			
Compared to DfnM	80	50	30
Compared to BaeI	85	54	27

Figure 13: DfnM and BaeI Compared to BaeI Homologs

Figure 14 shows the area of interest found within BaeI and DfnM. This sequence differed between the BaeI and DfnM sequences when compared to corresponding homologs. There is a question of if the histidine may have an influence on this area and have a part in creating distinct beta-branching types. This may be investigated in greater detail by others within the Reddick laboratory.

ClustalW of Area of Interest in BaeI and DfnM compared to BaeI and DfnM Homologs

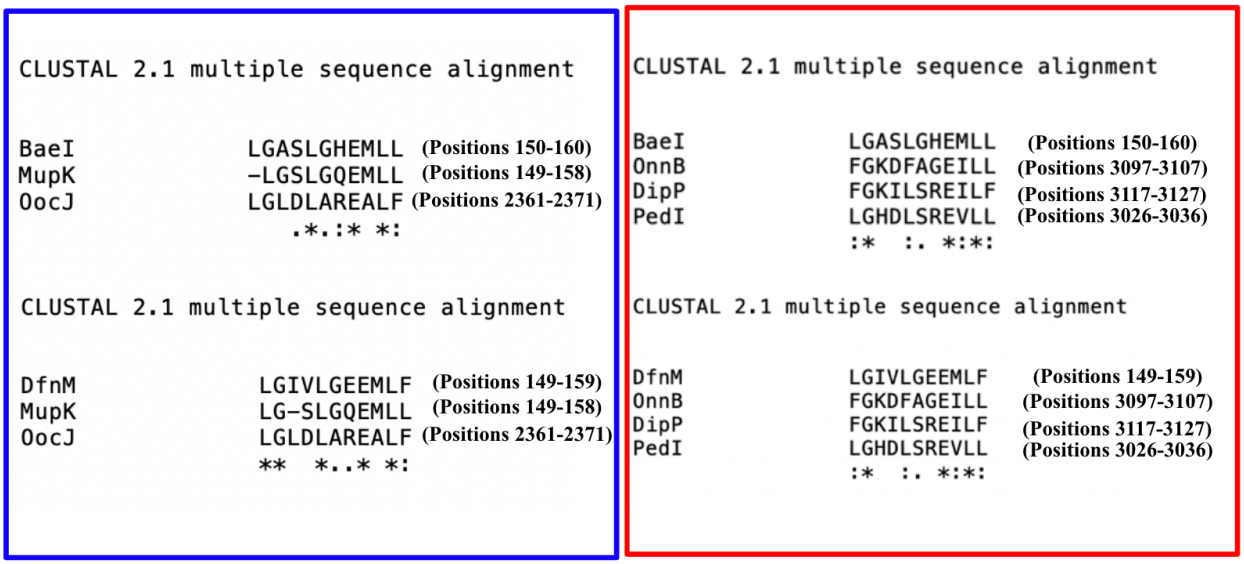

Figure 14: Area of Interest in BaeI and DfnM compared to BaeI and DfnM Homologs using ClustalW W Software

Conclusion and Future Work within the Reddick Laboratory.

Within these experiments, the PksL and BaeI genes have been purified and cloned into different vectors including Top10 and BL21Star. This prepares the genes to be used in future experiments to determine their roles in biosynthetic pathways. The reaction of PksL and coenzyme A are in the process of being analyzed and future work will be done to react PksL with other CoA enzymes such as Acetoacetyl-CoA. These experiments will allow the experimenters to determine if the formation of holo-S-PksL-T2 and Acetoacetyl-S-PksL-T2 is plausible using PksL. Homologs were found of BaeI and PksL and an area of interest was located within the gene sequence. The research group will continue to address the formation of the double bond within the structure of Difficidin and similar antibiotics.

References cited

(1) Geoffrey Siemering; Matthew Ruark; Amanda Gevens. The Value of Bacillus Amyloliquefaciens for Crop Production. University of Wisconsin System Board of Regents and University of Wisconsin-Extension, Cooperative Extension 2016.

(2) Polyketide and Nonribosomal Peptide Antibiotics: Modularity and Versatility - ProQuest http://search.proquest.com/docview/213603036 (accessed May 6, 2020).

(3) Afrin, S.; Bhuiyan, M. N. I. Antagonistic Activity of Bacillus Amyloliquefaciens Subsp. Amyloliquefaciens against Multidrug Resistant Serratia Rubidaea. *bioRxiv* **2019**, 818054. https://doi.org/10.1101/818054.

(4) Fan, B.; Blom, J.; Klenk, H.-P.; Borriss, R. Bacillus Amyloliquefaciens, Bacillus Velezensis, and Bacillus Siamensis Form an "Operational Group B. Amyloliquefaciens" within the B. Subtilis Species Complex. *Front. Microbiol.* **2017**, *8*. https://doi.org/10.3389/fmicb.2017.00022.

(5) DIFFICIDIN AND OXYDIFFICIDIN: NOVEL BROAD SPECTRUM ANTIBACTERIAL ANTIBIOTICS PRODUCED BY *BACILLUS SUBTILIS* https://www.jstage.jst.go.jp/article/antibiotics1968/40/12/40_12_1692/_article (accessed Aug 29, 2020).

(6) Chen, X.-H.; Vater, J.; Piel, J.; Franke, P.; Scholz, R.; Schneider, K.; Koumoutsi, A.; Hitzeroth, G.; Grammel, N.; Strittmatter, A. W.; Gottschalk, G.; Süssmuth, R. D.; Borriss, R. Structural and Functional Characterization of Three Polyketide Synthase Gene Clusters in Bacillus Amyloliquefaciens FZB 42. *J. Bacteriol.* **2006**, *188* (11), 4024–4036. https://doi.org/10.1128/JB.00052-06.

(7) Calderone, C. T.; Kowtoniuk, W. E.; Kelleher, N. L.; Walsh, C. T.; Dorrestein, P. C. Convergence of Isoprene and Polyketide Biosynthetic Machinery: Isoprenyl-S-Carrier Proteins in the PksX Pathway of Bacillus Subtilis. *Proc. Natl. Acad. Sci. U. S. A.* **2006**, *103* (24), 8977–8982. https://doi.org/10.1073/pnas.0603148103.

(8) Maloney, F. P.; Gerwick, L.; Gerwick, W. H.; Sherman, D. H.; Smith, J. L. Anatomy of the β-Branching Enzyme of Polyketide Biosynthesis and Its Interaction with an Acyl-ACP Substrate. *Proc. Natl. Acad. Sci. U. S. A.* **2016**, *113* (37), 10316–10321. https://doi.org/10.1073/pnas.1607210113.

(9) Walsh, C. T.; Fischbach, M. A. Natural Products Version 2.0: Connecting Genes to Molecules. *J. Am. Chem. Soc.* **2010**, *132* (8), 2469–2493. https://doi.org/10.1021/ja909118a.

(10) Calderone, C. T.; Iwig, D. F.; Dorrestein, P. C.; Kelleher, N. L.; Walsh, C. T. Incorporation of Non-Methyl Branches by Isoprenoid-Like Logic: Multiple β-Alkylation Events in the Biosynthesis of Myxovirescin A1. *Chem. Biol.* **2007**, *14* (7), 835–846. https://doi.org/10.1016/j.chembiol.2007.06.008.

(11) Becerril, A.; Pérez-Victoria, I.; Ye, S.; Braña, A. F.; Martín, J.; Reyes, F.; Salas, J. A.; Méndez, C. Discovery of Cryptic Largimycins in *Streptomyces* Reveals Novel Biosynthetic Avenues Enriching the Structural Diversity of the Leinamycin Family. *ACS Chem. Biol.* **2020**, *15* (6), 1541–1553. https://doi.org/10.1021/acschembio.0c00160.

(12) Ueoka, R.; Meoded, R. A.; Gran-Scheuch, A.; Bhushan, A.; Fraaije, M. W.; Piel, J. Genome Mining of Oxidation Modules in Trans-Acyltransferase Polyketide Synthases Reveals a Culturable Source for Lobatamides. *Angew. Chem. Int. Ed.* **2020**, *59* (20), 7761–7765. https://doi.org/10.1002/anie.201916005.

(13) Liang, H.; Jiang, L.; Jiang, Q.; Shi, J.; Xiang, J.; Yan, X.; Zhu, X.; Zhao, L.; Shen, B.; Duan, Y.; Huang, Y. A 3-Hydroxy-3-Methylglutaryl-CoA Synthase-Based Probe for the Discovery of the Acyltransferase-Less Type I Polyketide Synthases. *Environ. Microbiol.* **2019**, *21* (11), 4270–4282. https://doi.org/10.1111/1462-2920.14787.
(14) Sato, K.; Katsuyama, Y.; Yokota, K.; Awakawa, T.; Tezuka, T.; Ohnishi, Y. Involvement of β-Alkylation Machinery and Two Sets of Ketosynthase-Chain-Length Factors in the Biosynthesis of Fogacin Polyketides in Actinoplanes Missouriensis. *ChemBioChem* **2019**, *20* (8), 1039–1050. https://doi.org/10.1002/cbic.201800640.
(15) Gu, L.; Jia, J.; Liu, H.; Håkansson, K.; Gerwick, W. H.; Sherman, D. H. Metabolic Coupling of Dehydration and Decarboxylation in the Curacin A Pathway: Functional Identification of a Mechanistically Diverse Enzyme Pair. *J. Am. Chem. Soc.* **2006**, *128* (28), 9014–9015. https://doi.org/10.1021/ja0626382.
(16) PubChem. Bacillaene http://pubchem.ncbi.nlm.nih.gov/compound/25144999 (accessed Sep 26, 2020).
(17) PubChem. Weishanmycin A http://pubchem.ncbi.nlm.nih.gov/substance/406873028 (accessed Sep 26, 2020).
(18) PubChem. Guangnanmycin A http://pubchem.ncbi.nlm.nih.gov/substance/406873027 (accessed Sep 26, 2020).
(19) PubChem. Myxopyronin http://pubchem.ncbi.nlm.nih.gov/compound/136669146 (accessed Sep 26, 2020).
(20) PubChem. (2R)-N-[(S)-[(2S,4R,6R)-6-[(2S)-2,3-Dihydroxypropyl]-4-hydroxy-5,5-dimethyloxan-2-yl]-hydroxymethyl]-2-hydroxy-2-[(2R,5R,6R)-2-methoxy-5,6-dimethyl-4-methylideneoxan-2-yl]acetamide http://pubchem.ncbi.nlm.nih.gov/compound/132934247 (accessed Sep 26, 2020).
(21) PubChem. (E)-5-[(6Z,9E)-5-Acetyloxy-10-chloro-6-methyl-3-oxo-2,14-dioxabicyclo[11.2.1]hexadeca-6,9-dien-15-yl]-5-hydroxy-3-methylpent-3-enoic acid http://pubchem.ncbi.nlm.nih.gov/compound/15978563 (accessed Sep 26, 2020).
(22) PubChem. Batumin http://pubchem.ncbi.nlm.nih.gov/compound/197707 (accessed Sep 26, 2020).
(23) PubChem. Psymberin http://pubchem.ncbi.nlm.nih.gov/compound/11692946 (accessed Sep 26, 2020).
(24) PubChem. Phormidolide http://pubchem.ncbi.nlm.nih.gov/compound/101027923 (accessed Sep 26, 2020).
(25) PubChem. Malleilactone http://pubchem.ncbi.nlm.nih.gov/compound/136229184 (accessed Sep 26, 2020).
(26) PubChem. Difficidin http://pubchem.ncbi.nlm.nih.gov/compound/6438594 (accessed Sep 26, 2020).
(27) PubChem. Bongkrekic acid http://pubchem.ncbi.nlm.nih.gov/compound/6433556 (accessed Sep 26, 2020).
(28) PubChem. Leinamycin http://pubchem.ncbi.nlm.nih.gov/compound/9849230 (accessed Sep 26, 2020).
(29) Butcher, R. A.; Schroeder, F. C.; Fischbach, M. A.; Straight, P. D.; Kolter, R.; Walsh, C. T.; Clardy, J. The Identification of Bacillaene, the Product of the PksX Megacomplex in Bacillus Subtilis. *Proc. Natl. Acad. Sci. U. S. A.* **2007**, *104* (5), 1506–1509. https://doi.org/10.1073/pnas.0610503104.

(30) Yamada, T.; Hamada, M.; Floreancig, P.; Nakabachi, A. Diaphorin, a Polyketide Synthesized by an Intracellular Symbiont of the Asian Citrus Psyllid, Is Potentially Harmful for Biological Control Agents. *PLOS ONE* **2019**, *14* (5), e0216319. https://doi.org/10.1371/journal.pone.0216319.
(31) Chen, H.; Bian, Z.; Ravichandran, V.; Li, R.; Sun, Y.; Huo, L.; Fu, J.; Bian, X.; Xia, L.; Tu, Q.; Zhang, Y. Biosynthesis of Polyketides by Trans-AT Polyketide Synthases in Burkholderiales. *Crit. Rev. Microbiol.* **2019**, *45* (2), 162–181. https://doi.org/10.1080/1040841X.2018.1514365.
(32) Biggins, J. B.; Ternei, M. A.; Brady, S. F. Malleilactone, a Polyketide Synthase-Derived Virulence Factor Encoded by the Cryptic Secondary Metabolome of Burkholderia Pseudomallei Group Pathogens. *J. Am. Chem. Soc.* **2012**, *134* (32), 13192–13195. https://doi.org/10.1021/ja3052156.
(33) Helfrich, E. J. N.; Piel, J. Biosynthesis of Polyketides by Trans-AT Polyketide Synthases. *Nat. Prod. Rep.* **2016**, *33* (2), 231–316. https://doi.org/10.1039/C5NP00125K.
(34) Calderone, C. T. Isoprenoid-like Alkylations in Polyketide Biosynthesis. *Nat. Prod. Rep.* **2008**, *25* (5), 845–853. https://doi.org/10.1039/B807243D.
(35) Bertin, M. J.; Vulpanovici, A.; Monroe, E. A.; Korobeynikov, A.; Sherman, D. H.; Gerwick, L.; Gerwick, W. H. The Phormidolide Biosynthetic Gene Cluster: A Trans-AT PKS Pathway Encoding a Toxic Macrocyclic Polyketide. *ChemBioChem* **2016**, *17* (2), 164–173. https://doi.org/10.1002/cbic.201500467.
(36) B. McAlpine, J.; Chen, S.-N.; Kutateladze, A.; B. MacMillan, J.; Appendino, G.; Barison, A.; A. Beniddir, M.; W. Biavatti, M.; Bluml, S.; Boufridi, A.; S. Butler, M.; J. Capon, R.; H. Choi, Y.; Coppage, D.; Crews, P.; T. Crimmins, M.; Csete, M.; Dewapriya, P.; M. Egan, J.; J. Garson, M.; Genta-Jouve, G.; H. Gerwick, W.; Gross, H.; Kay Harper, M.; Hermanto, P.; M. Hook, J.; Hunter, L.; Jeannerat, D.; Ji, N.-Y.; A. Johnson, T.; I. Kingston, D. G.; Koshino, H.; Lee, H.-W.; Lewin, G.; Li, J.; G. Linington, R.; Liu, M.; L. McPhail, K.; F. Molinski, T.; S. Moore, B.; Nam, J.-W.; P. Neupane, R.; Niemitz, M.; Nuzillard, J.-M.; H. Oberlies, N.; M. Ocampos, F. M.; Pan, G.; J. Quinn, R.; Sai Reddy, D.; Renault, J.-H.; Rivera-Chávez, J.; Robien, W.; M. Saunders, C.; J. Schmidt, T.; Seger, C.; Shen, B.; Steinbeck, C.; Stuppner, H.; Sturm, S.; Taglialatela-Scafati, O.; J. Tantillo, D.; Verpoorte, R.; Wang, B.-G.; M. Williams, C.; G. Williams, P.; Wist, J.; Yue, J.-M.; Zhang, C.; Xu, Z.; Simmler, C.; C. Lankin, D.; Bisson, J.; F. Pauli, G. The Value of Universally Available Raw NMR Data for Transparency, Reproducibility, and Integrity in Natural Product Research. *Nat. Prod. Rep.* **2019**, *36* (1), 35–107. https://doi.org/10.1039/C7NP00064B.
(37) PubChem. Curacin A http://pubchem.ncbi.nlm.nih.gov/compound/5281967 (accessed Sep 27, 2020).
(38) PubChem. Byrostatin 1 http://pubchem.ncbi.nlm.nih.gov/substance/103513623 (accessed Sep 27, 2020).
(39) PubChem. 2-[[(2E,4E,6E,11R)-12-[(4As,6R,8S,8aR)-4-[[(2S)-2-hydroxy-2-[(2R,5R,6R)-2-methoxy-5,6-dimethyl-4-methylideneoxan-2-yl]acetyl]amino]-8-methoxy-7,7-dimethyl-4a,6,8,8a-tetrahydro-4H-pyrano[3,2-d][1,3]dioxin-6-yl]-11-hydroxydodeca-2,4,6-trienoyl]amino]-5-(diaminomethylideneamino)pentanoic acid http://pubchem.ncbi.nlm.nih.gov/compound/6438431 (accessed Sep 27, 2020).
(40) Buchholz, T. J.; Rath, C. M.; Lopanik, N. B.; Gardner, N. P.; Håkansson, K.; Sherman, D. H. Polyketide β-Branching in Bryostatin Biosynthesis: Identification of Surrogate Acetyl-

ACP Donors for BryR, an HMG-ACP Synthase. *Chem. Biol.* **2010**, *17* (10), 1092–1100. https://doi.org/10.1016/j.chembiol.2010.08.008.
(41) PubChem. 83314-01-6 http://pubchem.ncbi.nlm.nih.gov/substance/162012050 (accessed Oct 4, 2020).
(42) Fig. 1. Chemical structure of the antibiotic TA. TA is a macrocyclic... https://www.researchgate.net/figure/Chemical-structure-of-the-antibiotic-TA-TA-is-a-macrocyclic-polyketide-containing-an-a-b_fig1_12711062 (accessed Oct 4, 2020).
(43) (PDF) Genetic and functional analysis of genes required for the post-modification of the polyketide antibiotic TA of Myxococcus xanthus https://www.researchgate.net/publication/12711062_Genetic_and_functional_analysis_of_genes_required_for_the_post-modification_of_the_polyketide_antibiotic_TA_of_Myxococcus_xanthus (accessed Oct 4, 2020). https://doi.org/10.1099/00221287-145-11-3059.
(44) Simunovic, V.; Zapp, J.; Rachid, S.; Krug, D.; Meiser, P.; Müller, R. Myxovirescin A Biosynthesis Is Directed by Hybrid Polyketide Synthases/Nonribosomal Peptide Synthetase, 3-Hydroxy-3-Methylglutaryl–CoA Synthases, and Trans-Acting Acyltransferases. *ChemBioChem* **2006**, *7* (8), 1206–1220. https://doi.org/10.1002/cbic.200600075.
(45) Sucipto, H.; Sahner, J. H.; Prusov, E.; Wenzel, S. C.; Hartmann, R. W.; Koehnke, J.; Müller, R. In Vitro Reconstitution of α-Pyrone Ring Formation in Myxopyronin Biosynthesis. *Chem. Sci.* **2015**, *6* (8), 5076–5085. https://doi.org/10.1039/c5sc01013f.
(46) Nakabachi, A.; Ueoka, R.; Oshima, K.; Teta, R.; Mangoni, A.; Gurgui, M.; Oldham, N. J.; van Echten-Deckert, G.; Okamura, K.; Yamamoto, K.; Inoue, H.; Ohkuma, M.; Hongoh, Y.; Miyagishima, S.; Hattori, M.; Piel, J.; Fukatsu, T. Defensive Bacteriome Symbiont with a Drastically Reduced Genome. *Curr. Biol.* **2013**, *23* (15), 1478–1484. https://doi.org/10.1016/j.cub.2013.06.027.
(47) Piel, J.; Hui, D.; Wen, G.; Butzke, D.; Platzer, M.; Fusetani, N.; Matsunaga, S. Antitumor Polyketide Biosynthesis by an Uncultivated Bacterial Symbiont of the Marine Sponge Theonella Swinhoei. *Proc. Natl. Acad. Sci. U. S. A.* **2004**, *101* (46), 16222–16227. https://doi.org/10.1073/pnas.0405976101.
(48) (PDF) Polyketide assembly lines of uncultivated sponge symbionts from structure-based gene targeting https://www.researchgate.net/publication/24433517_Polyketide_assembly_lines_of_uncultivated_sponge_symbionts_from_structure-based_gene_targeting (accessed Oct 4, 2020). https://doi.org/10.1038/nchembio.176.
(49) type I polyketide synthase, PedI-like protein [Candidatus Profftella a - Protein - NCBI https://www-ncbi-nlm-nih-gov.libproxy.uncg.edu/protein/527122298 (accessed Oct 4, 2020).
(50) occR (plasmid) [Agrobacterium tumefaciens] - Protein - NCBI https://www-ncbi-nlm-nih-gov.libproxy.uncg.edu/protein/AAA98378.1 (accessed Oct 4, 2020).
(51) OnnB [symbiont bacterium of Theonella swinhoei] - Protein - NCBI https://www-ncbi-nlm-nih-gov.libproxy.uncg.edu/protein/AAV97870.1 (accessed Oct 4, 2020).
(52) ACP S-malonyltransferase [Burkholderia thailandensis] - Protein - NCBI https://www-ncbi-nlm-nih-gov.libproxy.uncg.edu/protein/497579874 (accessed Oct 4, 2020).
(53) Overview: malL, Burkholderia thailandensis E264 ATCC 700388 https://burkholderia.com/feature/show?id=384776 (accessed Oct 4, 2020).

(54) BryR [Candidatus Endobugula sertula] - Protein - NCBI https://www-ncbi-nlm-nih-gov.libproxy.uncg.edu/protein/ABM63533.1 (accessed Oct 4, 2020).
(55) polyketide synthase [Serratia plymuthica] - Protein - NCBI https://www-ncbi-nlm-nih-gov.libproxy.uncg.edu/protein/AFX60332.1 (accessed Oct 11, 2020).
(56) RecName: Full=Trans-enoyl reductase phmE; AltName: Full=Phomacin biosy - Protein - NCBI https://www-ncbi-nlm-nih-gov.libproxy.uncg.edu/protein/Q0V6Q3.2 (accessed Oct 11, 2020).
(57) Eustáquio, A. S.; Janso, J. E.; Ratnayake, A. S.; O'Donnell, C. J.; Koehn, F. E. Spliceostatin Hemiketal Biosynthesis in Burkholderia Spp. Is Catalyzed by an Iron/α-Ketoglutarate–Dependent Dioxygenase. *Proc. Natl. Acad. Sci.* **2014**, *111* (33), E3376–E3385. https://doi.org/10.1073/pnas.1408300111.
(58) Ishida, K.; Lincke, T.; Hertweck, C. Assembly and Absolute Configuration of Short-Lived Polyketides from Burkholderia Thailandensis. *Angew. Chem. Int. Ed.* **2012**, *51* (22), 5470–5474. https://doi.org/10.1002/anie.201200067.
(59) Lopanik, N. B.; Shields, J. A.; Buchholz, T. J.; Rath, C. M.; Hothersall, J.; Haygood, M. G.; Håkansson, K.; Thomas, C. M.; Sherman, D. H. In Vivo and in Vitro Trans-Acylation by BryP, the Putative Bryostatin Pathway Acyltransferase Derived from an Uncultured Marine Symbiont. *Chem. Biol.* **2008**, *15* (11), 1175–1186. https://doi.org/10.1016/j.chembiol.2008.09.013.
(60) Piel, J.; Wen, G.; Platzer, M.; Hui, D. Unprecedented Diversity of Catalytic Domains in the First Four Modules of the Putative Pederin Polyketide Synthase. *Chembiochem Eur. J. Chem. Biol.* **2004**, *5* (1), 93–98. https://doi.org/10.1002/cbic.200300782.
(61) Piel, J. A Polyketide Synthase-Peptide Synthetase Gene Cluster from an Uncultured Bacterial Symbiont of Paederus Beetles. *Proc. Natl. Acad. Sci. U. S. A.* **2002**, *99* (22), 14002–14007. https://doi.org/10.1073/pnas.222481399.
(62) Song, L.; Jenner, M.; Masschelein, J.; Jones, C.; Bull, M. J.; Harris, S. R.; Hartkoorn, R. C.; Vocat, A.; Romero-Canelon, I.; Coupland, P.; Webster, G.; Dunn, M.; Weiser, R.; Paisey, C.; Cole, S. T.; Parkhill, J.; Mahenthiralingam, E.; Challis, G. L. Discovery and Biosynthesis of Gladiolin: A Burkholderia Gladioli Antibiotic with Promising Activity against Mycobacterium Tuberculosis. *J. Am. Chem. Soc.* **2017**, *139* (23), 7974–7981. https://doi.org/10.1021/jacs.7b03382.
(63) putative type I polyketide synthase [symbiont bacterium of Paederus fu - Protein - NCBI https://www-ncbi-nlm-nih-gov.libproxy.uncg.edu/protein/38374225 (accessed Oct 30, 2020).
(64) PKS [Leptolyngbya sp. ISBN3-Nov-94-8] - Protein - NCBI https://www-ncbi-nlm-nih-gov.libproxy.uncg.edu/protein/AMH40443.1 (accessed Oct 30, 2020).
(65) PubChem. Thiomarinol http://pubchem.ncbi.nlm.nih.gov/compound/5825095 (accessed Sep 27, 2020).
(66) baeI [Bacillus amyloliquefaciens CC178] - Protein - NCBI https://www-ncbi-nlm-nih-gov.libproxy.uncg.edu/protein/AGZ56441.1 (accessed Nov 24, 2020).
(67) DfnM [Bacillus velezensis UCMB5113] - Protein - NCBI https://www-ncbi-nlm-nih-gov.libproxy.uncg.edu/protein/CDG26412.1 (accessed Nov 24, 2020).
(68) MupK [Pseudomonas fluorescens] - Protein - NCBI https://www-ncbi-nlm-nih-gov.libproxy.uncg.edu/protein/AAM12924.1 (accessed Nov 24, 2020).

(69) type I polyketide synthase, PedI-like protein [Candidatus Profftella a - Protein - NCBI https://www-ncbi-nlm-nih-gov.libproxy.uncg.edu/protein/527122298 (accessed Nov 24, 2020).
(70) Moebius, N.; Ross, C.; Scherlach, K.; Rohm, B.; Roth, M.; Hertweck, C. Biosynthesis of the Respiratory Toxin Bongkrekic Acid in the Pathogenic Bacterium Burkholderia Gladioli. *Chem. Biol.* **2012**, *19* (9), 1164–1174. https://doi.org/10.1016/j.chembiol.2012.07.022.
(71) Fisch, K.; Gurgui, C.; Heycke, N.; Sar, S.; Anderson, S.; Webb, V.; Taudien, S.; Platzer, M.; Rubio, B.; Robinson, S.; Crews, P.; Piel, J. Polyketide Assembly Lines of Uncultivated Sponge Symbionts from Structure-Based Gene Targeting. *Nat. Chem. Biol.* **2009**, *5*, 494–501. https://doi.org/10.1038/nchembio.176.
(72) Walker, P. D.; Williams, C.; Weir, A. N. M.; Wang, L.; Crosby, J.; Race, P. R.; Simpson, T. J.; Willis, C. L.; Crump, M. P. Control of β-Branching in Kalimantacin Biosynthesis: Application of 13 C NMR to Polyketide Programming. *Angew. Chem. Int. Ed Engl.* **2019**, *58* (36), 12446–12450. https://doi.org/10.1002/anie.201905482.
(73) PubChem. Oocydin A http://pubchem.ncbi.nlm.nih.gov/compound/15978563 (accessed Nov 24, 2020).
(74) PubChem. Onnamide http://pubchem.ncbi.nlm.nih.gov/compound/10373128 (accessed Nov 24, 2020).
(75) PubChem. Diaphorin http://pubchem.ncbi.nlm.nih.gov/compound/132934247 (accessed Nov 24, 2020).
(76) JamJ [Lyngbya majuscula] - Protein - NCBI https://www-ncbi-nlm-nih-gov.libproxy.uncg.edu/protein/AAS98781.1 (accessed Nov 24, 2020).
(77) CurF [Lyngbya majuscula] - Protein - NCBI https://www-ncbi-nlm-nih-gov.libproxy.uncg.edu/protein/AAT70101.1 (accessed Nov 24, 2020).
(78) hybrid trans-AT polyketide synthase - nonribosomal peptide synthetase - Protein - NCBI https://www-ncbi-nlm-nih-gov.libproxy.uncg.edu/protein/282554962 (accessed Nov 24, 2020).